



NANOSTRUCTURED IRREGULARITY STUDY BY X-RAY SMALL-ANGLE SCATTERING

**V. P. SELYAEV, R. E. NURLYBAEV*, V. A. NEVEROV,
S. B. AIDAROVA, M. T. ZHUGINISOV and A. A. MURZAGULOVA**

KazNTU Named After K. I. Satpayev, Satpayev St. 22, 050013,
ALMATY, KAZAKHSTAN

ABSTRACT

X-ray small-angle scattering and structural nanometer level irregularities of dispersed natural diatomite particles of some Aktobe region deposits, Kazakhstan. The pore structure parameters and fractal characteristics of scatter formations have been determined. Fractal dimensions of particles from the Middle Volga region diatomite deposits, the Russian Federation, are given below.

Key words: Diatomite, Irregularity, X-ray small-angle scattering, Fractal dimension.

INTRODUCTION

Small-angle X-ray scattering (SAXS) is a diffraction method widely used for the study of nano-objects of different physical nature and aggregation state, including superfine powders. The most important feature of this method is the ability to analyze the internal structure of disordered systems. From this point of view, its application is the way to receive direct structural information on systems with a random distribution of micro-nano-level irregularities^{1,2}. Patterns of small-angle scattering is the result of X-ray interference coherently scattered on a test sample. When the 0.05-0.5 nm X-ray wave length being from, the X-ray small-angle scattering method enables to investigate structures of size from a few to several hundred nanometers. The pattern of interference scattering is formed by adding a number of secondary coherently scattered waves that differ from each other in phase. The phase difference and amplitude of composed waves depend on spatial electron density distribution, i.e. on a studied object structure, which determines the experimental scattering curve shape $I(s)$, where s – a scattering vector. Its modulus is defined by the relation $s = 4\pi \sin \theta / \lambda$ (2θ – a scattering angle; λ – the X-ray wavelength). So a small-angle scattering intensity with the N particle assembly (irregularities of electron density), placed in a

* Author for correspondence; E-mail: bagdat777_87@mail.ru

homogeneous medium (a solid matrix or solvent), characterized by spatial scattering density distribution ρ can be written as³.

$$I(s) = nF(s) K(s) \quad \dots(1)$$

where $n = N/V$ – irregularities concentration; $F(s)$ – a form factor of scattering irregularities, depending on their shape, structure and contrast – i.e. the difference between mean scattering density of irregularities and the scattering density of surrounding matrix – $\Delta\rho = \rho(r) - \rho$. Parameter $K(s)$ – an effective structural factor. It should be noted that a $\Delta\rho$ contrast is the most important parameter that determines the small-angle scattering method effectiveness. If the Guinier condition is satisfied – $sR < 1$, $K(s) = 1$ – then the scattering is determined as a set of spherical shape irregularities with typical dimensions $\langle R \rangle$ and the small-angle scattering intensity drop will be defined by the formula

$$I(s) = I(0) \exp(-s^2 R_g^2 / 3) \quad \dots(2)$$

The analysis of scattering in a Guinier mode enables to estimate by the rate of curves $\log I(s) - s^2$ the radius of gyration of irregularities R_g and their typical dimensions, which in this case⁴ are defined by relation –

$$\langle R \rangle = (5/3)^{1/2} R_g. \quad \dots(3)$$

If the $sR > 1$ condition is satisfied there one can see A Porod's scattering mode¹, where the intensity dependence $I(s)$ on a scattering vector module s is of a degree character $I(s) \sim s^{-f}$, where $f \leq 6$. The value of this parameter enables to speak about possible fractality of the system (mass fractals, fractal surfaces). If the Porod's law ($f=4$) is satisfied then scattering takes place on spherical shape smooth surface particles of almost the same size (irregularities). So, obtaining the exponent value m from a slope of tangent sections of the X-ray small-angle scattering curve, built in double logarithmic coordinates ($\log(I(s)) - \log s$), enables to define the type of fractal (mass or surface) and the size of fractal dimension $D = f$ for a mass fractal and $D_s = 6 - f$ – for the surface fractal^{1,3}. The distribution of mass in space for mass fractals (pores, clusters of irregularities) depends on its size r –

$$M(r) = M_0 r^D, (r_0 < r < R) \quad \dots(4)$$

At this, the exponent D coincides with fractal dimension – $1 \leq D \leq 3$. For lined up spherical irregularities (pore channels) $D = 1$; for a curved chain of spheres $1 < D < 2$; for rose type gravels⁵ $D = 3$. In the case of facing a scattering from a three-dimensional fractal surface object (phase interface), the area measured in r scale will be equal to –

$$S(r) = r^2 (R/r)^{D_s} \quad \dots(5)$$

and the exponent $f = 6 - D_s$, where D_s – a fractal dimension of the surface is in the range of $2 \leq D_s < 3$, with $3 < f \leq 4$. For flaw less surfaces $D_s = 2$, $f = 4$ – the Porod's law¹.

Diatomite is a light, porous, sedimentary rock composed mainly by siliceous shell fragments of aquatic plants (diatoms) and consisting mainly of silica hydrates of various degrees – a kind of Opal $m\text{SiO}_2 \cdot n\text{H}_2\text{O}$.^{6,7} The size of diatom flaps (shells) usually ranges from 0.03 to 0.15 mm and the content of SiO_2 – from 62 to 97%. They usually consist of constant impurities: clay minerals (~ 5...10%) consisting of fine less than 0.01 mm particles that are ductile, heat-resistant and characterized by absorption and water retention properties. At this SiO_2 particles according to generation conditions in natural environment can differ in linear size, porosity degree and structural irregularity. Paper⁸ shows that individual spherical silica particles of size ~ 225 nm and particle druses of size ~ 20...40 nm demonstrate the inner substructure presented by primary 5...10 nm particles that generate a ~ 300...500 nm core⁹. The core is surrounded by shells made of secondary ~ 20...40 nm size particles (composed of primary particles), alternating with primary particle layers. If to assume that a core of dispersed microsilica particles is composed of primary particles – 5...10 nm size balls, then at a tetrahedral packing of particles there are being generated the $0.225d$ linear dimension pores, where d – a diameter of balls, at an octahedral method of particle packing the diameter of balls is equal to $0.414d$.

Consequently, the core of a amorphous silica particle also including secondary particles has 1.1...2.3 nm size pores at tetrahedral packing) and 2.1...4.1 nm size pores at octahedral packing. According to the shell structure of silica particles^{9,10}, the core is surrounded by several layers of secondary 20...40 nm size particles. At a tetrahedral secondary particles packing there are expected to appear 4.5...9.0 nm size pores, while at an octahedral packing the pores will be of size 8.3...16.7 nm. Thus, submicron dispersed microsilica particles should have a pore structure with a linear size of pores ranging from 1.1...16.7 nm. But in reality, the upper limit of pore diameters may be a bit higher due to particle packing defects and deviations of the shape of primary and secondary particles from the spherical one. Tertiary silica particles consisting of a core and secondary ~500 nm size particles can have porous space up to 100...200 nm.

The purpose of this study was in defining basic characteristics of nano-sized structure irregularities in natural diatomite particles developed in some Aktobe region deposits of Kazakhstan, a very perspective material in construction and chemical industries. The other purpose of the paper was in making a comparative data analysis of disperse systems and natural diatomite parameters developed at the Middle Volga region deposits, the Russian Federation, previously studied in¹¹⁻¹³.

EXPERIMENTAL

Natural diatomite from Utesaysky, Zhalpaksy and Kirgyzsky from Aktobe region deposits in Kazakhstan is a sedimentary rock, slightly cemented, grey-yellowish with ~ 250 - 1000 nm fine postgrinding particles. The experimental data in the form of X-ray small-angle scattering curves were obtained by the Hecus company small-angle diffractometer. There was used $\text{CuK}\alpha$ - radiation ($\lambda = 1.5418 \text{ \AA}$) and Ni- filter. Scattering intensities were recorded in the range of scattering vectors s 0.007 - 0.600 \AA^{-1} . Adjusted for a range of scattering vectors and dependencies of linear dimensions of structural inhomogeneities $\delta \sim 2\pi/s$, this experimental material allows to register nanoobjects of size 1 - 90 nm. Fig. 1 shows experimental dependence of the X-ray small-angle scattering intensity in double logarithmic coordinates on samples of natural diatomite from Utesaysky, Zhalpaksy, Kirgyzsky deposits, Aktobe region, Kazakhstan. Scattering curves of all three powders are symbate besides a common feature for the samples under study is the character of scattering and a presence of corresponding curves of different vector intervals s , in which the type or behavior of the dependence $I(s)$ differs substantially. In the range of scattering vector values Δs 0.027 - 0.054 \AA^{-1} and 0.100 - 0.200 \AA^{-1} the behavior of $I(s)$ obeys a degree law s^{-f} for all three investigated diatomites.

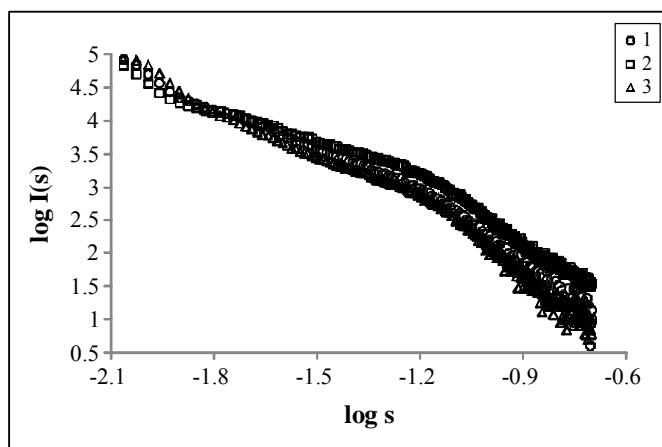


Fig. 1: X-ray small-angle scattering curves, Utesaysky - 1 Zhalpaksy – 2, Kirgyzsky - 3 deposits

The f exponents have been determined from the slope of straight experimental curve sections $\log I(s) - \log s$. Fig. 2 shows a scattering indicatrix portion for a range of vectors s 0.027 - 0.054 \AA^{-1} . f parameter values for powders from Utesaysky, Zhalpaksy, Kirgyzsky diatomite deposits are equal to 1.99 , 1.48 and 1.88 , which corresponds to a scattering by

inhomogeneities with a mass-fractal³ aggregation – clusters – with fractal size $D = f$ 1.99, 1.48 and 1.88.

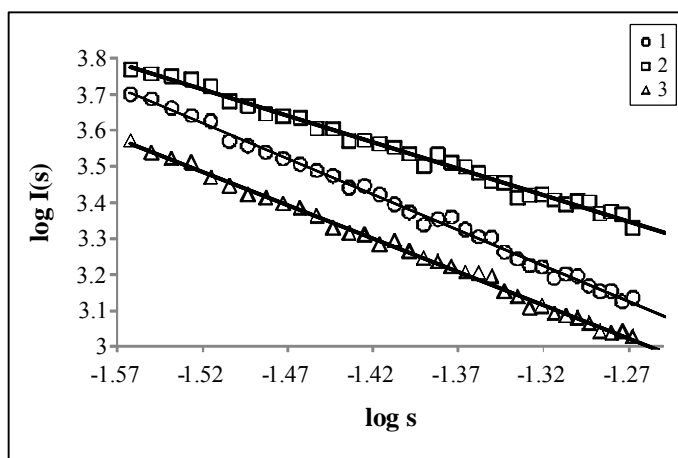


Fig. 2: Dependencies $\log I(s) - \log s$ of diatomite deposits, Utesaysky - 1 Zhalpaksy - 2, Kyrgyzsky - 3 for a range of vectors s $0.027 - 0.054 \text{ \AA}^{-1}$

This type of clusters may be greatly curved sphere-like chain inhomogeneities, particularly, they are porous channels, as well as voluminous fractal nature aggregates. The scale size of indicated irregularities, calculated from the range value of boundaries of scattering vector variation is $\sim 23\text{-}12 \text{ nm}$, and it may well correspond to fragments of the pore system at amorphous silica particles⁹. The difference in fractal characteristics of nanoscale inhomogeneities in investigated diatomite is probably connected with specific generation conditions of diatom shells from respective territorial deposits^{6,14}.

Fractal scattering mode is found from the slope of straight sections in experimental curves (in double logarithmic coordinates) of dispersed powders in a range of vectors s $0.100\text{-}0.200 \text{ \AA}^{-1}$ - Fig. 3. Calculated values f are equal to 3.77 for scattering material from Utesaysky deposit; 3.22 - for Zhalpaksy scattering material and 3.78 for the Kyrgyzsky deposit scattering material.

The size scale of scattering irregularities makes up $\sim 6\text{-}3 \text{ nm}$. Since in this case the condition $sR > 1$ is satisfied, then there is seen the Porod's mode scattering on fractal surfaces with their fractal dimensions being equal to $D_s = 6 - f$. Thus, the particles of investigated diatomite incorporate structural irregularities in the form of fractal surfaces (interfaces, such as time - silica solid phase) with fractal dimensions: Utesaysky deposit - $D_s = 2.23$; Zhalpaksy - $D_s = 2.78$; Kyrgyzsky - $D_s = 2.22$.

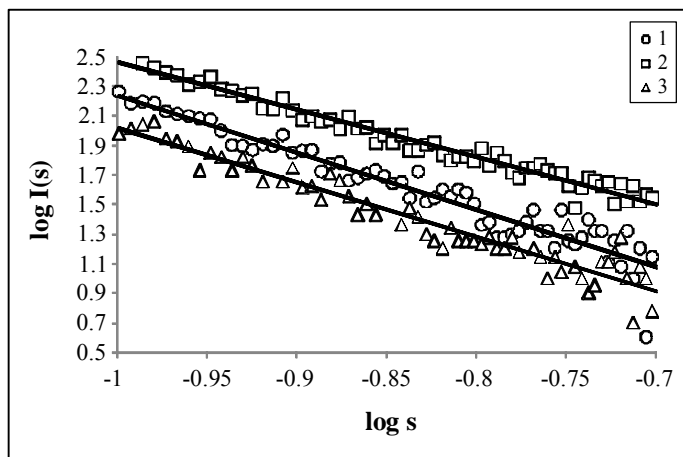


Fig. 3: Dependencies $\log I(s) - \log s$ diatomite deposits from Utesaysky – 1, Zhalpaksky – 2, Kyrgyz - 3 for a range of vectors s $0.100 - 0,200 \text{ \AA}^{-1}$.

A detailed analysis of scattering curves behavior revealed that the deviation from the power law s^{-f} is observed in small and high values of scattering vectors. For small values s means the deviation that may be connected with the yield to a Guinier scattering mode, where, as shown in^{1,3}, a curve shape $I(s) - s^{-2}$ is defined by a typical size R of independently scattering fractal clusters. But investigated diatomite powders are polydisperse systems-amorphous silica particles having a complex pore structure¹⁰ with linear pore size $1 \sim 20 \text{ nm}$ (and more), that explains the absence of straight sections typical for monodisperse systems in the field of small scattering vector values s on the curves $\log I(s) - s^{-2}$. In the region of large scattering vectors $I(s)$ ceases to depend on s , which is probably due to incoherent scattering on structural less than 3 nm irregularities. So it means that characterization of fractal $3\text{-}1 \text{ nm}$ clusters scale does not seem possible.

But when a Guinier scattering mode is not performed then one can value the radii of gyration of structural irregularities by the linear connection $\{s^2 I(s) - s\}$ (graphics Kratky)¹⁵, Fig. 4. The maximum angle of the Kratky graphics enables to assess the average radii of gyration $\langle R_g \rangle$ of scattering structures (here-pores or their clusters). From the Guinier relation (2) it follows¹⁵ that $\langle R_g \rangle^2 = 3/s_{\max}^2$, where s_{\max} – the Kratky graph maximum angle. Graphics processing results see in Table 1. The values of $\langle R \rangle$ are defined by the formula (3).

The Table shows that the average linear dimensions of structural diatomite particle irregularities studied have similar values and are quite consistent with papers^{9,10} data in the framework of the shell model of the amorphous silica particles structure.

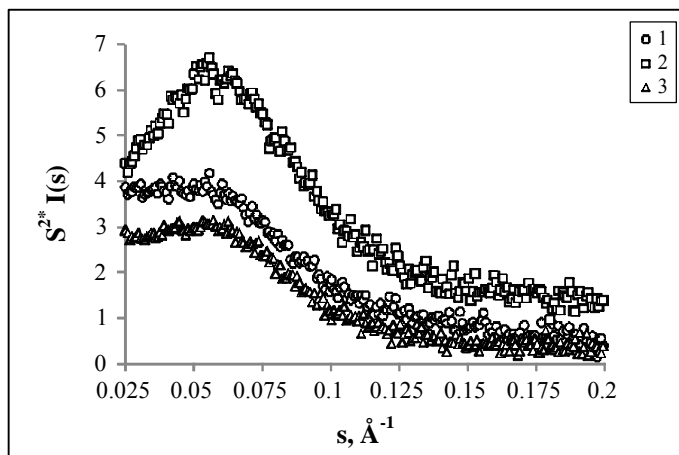


Fig. 4: Kratky graphics for diatomite deposits from Utesaysky – 1, Zhalpaksky – 2, Kyrgyzsky - 3

Table 1

Deposit	s_{\max} (\AA^{-1})	$\langle R_g \rangle$ (nm)	$\langle R \rangle$ (nm)
Utesaysky	0.052	3.3	4.3
Zhalpaksky	0.057	3.0	3.9
Kyrgyzsky	0.055	3.1	4.0

Table 2 shows fractal dimensions of the Kazakhstan structural irregularities of some diatomites investigated and of those taken from the Middle Volga region deposits, the Russian Federation, see¹¹⁻¹³. Note that in this case the diatomite deposits specified in Table 2 have similar fractal characteristics.

Table 2

Deposit	D	D _s
Utesaysky	1.99	2.23
Zhalpaksky	1.48	2.78
Kyrgyzsky	1.88	2.22
Atemarsky	1.56	2.27
Inzensky	1.73	–
Nikolsky	1.07	2.28

So particles of Zhalpaksy diatomite have most rough and rugged surface and nanoscale scale irregularities of Inzensky diatomite have fractal surfaces.

CONCLUSION

- (i) X-ray small-angle scattering can be used for the analysis of structural nanoscale irregularity features of dispersed material particles and mineral powders.
- (ii) It was found that the particles of Kazakhstan diatomite deposits have structural irregularities in the form of fractal porous system clusters within the frame of a amorphous silica particle shell model as well as the fractal pore-solid body surfaces.
- (iii) In general Kazakhstan and Russia diatomite deposits have similar structural characteristics of nanolarge particles.
- (iv) The results may be useful for the prediction of thermo-physical properties of fillers for vacuum insulation products made on the basis of dispersed silica structures.

REFERENCES

1. D. I. Svergun and L. A. Feigin, X-ray and Neutron Small-angle Scattering, - M.: Nauka. Ch. Ed. Phys. Mat. Lighted, 280 (1986).
2. V. P. Selyaev and V. A. Neverov, Apparatus and Methods of Disperse Systems, Innovative Education, **4(7)**, S. 71-120 (2013).
3. T. V. Khamova, O. A. Shilov, G. P. Kopice, Opole Voivodeship, L. Almasy and L. Rosta, Research Mesostructure Bioactive Coatings for Stone Materials Based on Epoxy-called Sols Siloxane-modified Nanodiamond by Small Angle Neutron Scattering, Solid State body, **56(1)**, 107-115 (2014).
4. C. M. Sorensen and Shi D. Guiner, Analysis for Homogeneous Dielectric Spheres of Arbitrary Size, Optics Communications, **178**, 31-36 (2000).
5. T. N. Vasilevskaya and T. V. Antropova, Study of the Structure of Nanoporous Glassy Matrices by X-ray Small-angle Scattering, Solid State Physics, T. 51, **12**, S. 2386-2393 (2009).
6. U. G. Distanov, Siliceous Rocks of the USSR/U. G. Distanov, Kazan: Tatar Publishing House (1976) p. 412.

7. V. P. Selyaev, V. A. Neverov, L. I. Kupriyashkina, A. V. Kolotushkin and V. V. Sidorov, Microstructure Promising Heat-insulating Materials on the Basis of Diatomite Middle Volga, *Regional Architecture and Engg.*, **1**, 12-18 (2013).
8. I. A. Karpov, E. N. Samara, V. M. Masalov, S. I. Bozhko et al., On the Internal Structure of Spherical Particles Opal, *Solid State Physics*, T. 47, **2**, S. 334-338 (2005).
9. V. M. Masalov, N. S. Suhinina and G. A. Emelchenko, Nanostructure Silica Particles Obtained by Multi-stage Shtobera-Finca Bona, *HFTP*, **2(4)**, S. 373-384 (2011).
10. V. A. Neverov, K. N. Nishchev, V. P. Selyaev and A. A. Panov, Study the Nanostructure of Condensed Silica Fume by Small-angle X-ray Scattering, *Appl. Phys.*, **4**, 38-42 (2013).
11. V. P. Selyaev, V. A. Neverov, L. I. Kupriyashkina, A. K. Osipov and O. A. Udina, Diatomite Middle Volga, Structure and Properties, Science, Technology and Higher Education: Materials of the II International Research and Practice Conference, Vol. II. April 17th, Westwood, Canada (2013) pp. 218-227.
12. V. P. Selyaev, V. A. Neverov, O. G. Mashtaev and A. V. Kolotushkin, Properties of Silica Fume from Natural Diatomite and its Application in the Manufacture of Vacuum Insulated Panels, *Civil Engg. J.*, **7**, 15-25 (2013).
13. V. P. Selyaev, V. A. Neverov and L. I. Kupriyashkina, Prediction of Heat Conduction and Evaluation of the Structural Characteristics of Granular Systems to Create a New Generation of Thermal Insulation Materials, *Academia, Architecture and Construction*, **1**, S. 89-93 (2014).
14. I. N. Demidov and T. S. Shelekhova, Diatomite Karelia (Especially the Formation, Distribution, use Prospects), Petrozavodsk: Karelian Research Centre, 89 (2006).
15. T. N. Vasilevskaya and R. I. Zakharchenya, The Structure of Nanocrystalline γ -Modification of Aluminum Oxide Doped with Chromium Cations (γ -Al₂O₃: Cr), According to X-ray Scattering at Small and Medium-sized Angles, *Solid State Physics*, **38(10)**, S. 3129-3143 (1996).

Accepted : 19.06.2015